



1 **Large salinity gradient and diagenetic changes in the northern**
2 **Indian Ocean dominate the stable oxygen isotopic variation in**
3 ***Globigerinoides ruber***
4

5 Rajeev Saraswat^{1*}, Thejasino Suokhrie¹, Dinesh K. Naik², Dharmendra P. Singh³, Syed M.
6 Saalim⁴, Mohd Salman¹, Gavendra Kumar¹, Sudhira R. Bhadra¹, Mahyar Mohtadi⁵, Sujata R.
7 Kurtarkar¹, Abhayanand S. Maurya³

8 ¹ Micropaleontology Laboratory, National Institute of Oceanography, Goa, India

9 ² Banaras Hindu University, Varanasi, Uttar Pradesh, India

10 ³ Indian Institute of Technology, Roorkee, India

11 ⁴ National Center for Polar and Ocean Research, Goa, India

12 ⁵ MARUM, University of Bremen, Bremen, Germany

13 * Correspondence to: Rajeev Saraswat (rsaraswat@nio.org)

14

15 **Abstract.** The application of stable oxygen isotopic ratio of surface dwelling *Globigerinoides ruber* (white variety)
16 ($\delta^{18}\text{O}_{ruber}$) to reconstruct past hydrological changes requires precise understanding of the effect of ambient parameters
17 on $\delta^{18}\text{O}_{ruber}$. The northern Indian Ocean, with huge freshwater influx and being a part of the Indo-Pacific Warm Pool,
18 provides a unique setting to understand the effect of both the salinity and temperature on $\delta^{18}\text{O}_{ruber}$. Here, we use a total
19 of 400 surface samples (252 from this work and 148 from previous studies), covering the entire salinity end member
20 region, to assess the effect of seawater salinity and temperature on $\delta^{18}\text{O}_{ruber}$ in the northern Indian Ocean. The analyzed
21 surface $\delta^{18}\text{O}_{ruber}$ very well mimics the expected $\delta^{18}\text{O}$ calcite estimated from the modern seawater parameters
22 (temperature, salinity and seawater $\delta^{18}\text{O}$). We report a large diagenetic overprinting of $\delta^{18}\text{O}_{ruber}$ in the surface
23 sediments with an increase of 0.18‰ per kilometer increase in water depth. The salinity exerts the major control on
24 $\delta^{18}\text{O}_{ruber}$ ($R^2 = 0.63$) in the northern Indian Ocean, with an increase of 0.29‰ per unit increase in salinity. The
25 relationship between temperature and salinity corrected $\delta^{18}\text{O}_{ruber}$ ($\delta^{18}\text{O}_{ruber} - \delta^{18}\text{O}_{sw}$) in the northern Indian Ocean [$T =$
26 $-0.59 * (\delta^{18}\text{O}_{ruber} - \delta^{18}\text{O}_{sw}) + 26.40$] is different than reported previously based on the global compilation of plankton
27 tow $\delta^{18}\text{O}_{ruber}$ data. The revised equations will help in better paleoclimatic reconstruction from the northern Indian
28 Ocean.
29



30 1. Introduction

31 The stable oxygen isotopic ratio ($\delta^{18}\text{O}$) of biogenic carbonates is one of the most extensively used marine paleoclimatic
32 proxies (Mulitza et al., 1997; Lea, 2014; Metcalfe et al., 2019; Saraswat et al., 2019). Even though it was initially
33 suggested that the oxygen isotopic fractionation in biogenic carbonates is largely driven by temperature (Urey et al.,
34 1947), subsequent work revealed that besides temperature, salinity and carbonate ion concentration of ambient
35 seawater also affect the biogenic carbonate $\delta^{18}\text{O}$ (Vergnaud-Grazzini, 1976; Spero et al., 1997; Bemis et al., 1998;
36 Spero et al., 1997; Bijma et al., 1999; Mulitza et al., 2003). On longer time-scales, the global ice volume contributes
37 the largest fraction (~1.0-1.2‰) of the glacial-interglacial shift in marine biogenic carbonate $\delta^{18}\text{O}$, at a majority of the
38 locations (Shackleton, 1987; 2000; Lambeck et al., 2014). The ice volume changes induced well-defined shifts in
39 biogenic carbonate $\delta^{18}\text{O}$ during the last several million years. Therefore, the regional evaporation-precipitation, runoff
40 and temperature changes are reconstructed from the global ice-volume corrected biogenic carbonate $\delta^{18}\text{O}$ (Saraswat
41 et al., 2012; 2013; Kessarkar et al., 2013).

42 The $\delta^{18}\text{O}$ of surface dwelling planktic foraminifera *Globigerinoides ruber* ($\delta^{18}\text{O}_{ruber}$) is often used to
43 reconstruct past surface seawater conditions (Saraswat et al., 2012; 2013; Mahesh and Banakar, 2014). The
44 relationship between $\delta^{18}\text{O}_{ruber}$ and ambient seawater physico-chemical conditions, however, varies from basin to basin
45 (Vergnaud-Grazzini, 1976; Mulitza et al., 2003; Horikawa et al., 2015; Hollstein et al., 2017). Therefore, continuous
46 efforts are made to understand the regional factors affecting $\delta^{18}\text{O}_{ruber}$ (Mulitza et al., 1997; 2003; Mohtadi et al., 2011;
47 Hollstein et al., 2017). The northern Indian Ocean being influenced by huge fresh water influx as well as being a part
48 of the Indo-Pacific Warm Pool (De Deckker, 2016), provides a unique setting to understand the effect of large salinity
49 and temperature changes on $\delta^{18}\text{O}_{ruber}$. Earlier, Duplessy et al., (1981) measured $\delta^{18}\text{O}$ of the living *G. ruber* specimens
50 collected from the water column as well as of the dead ones recovered from surface sediments of the northern Indian
51 Ocean. A similar study from the Red Sea and adjoining western Arabian Sea suggested that *G. ruber* calcifies its test
52 in isotopic equilibrium with the ambient seawater, thus tracking the inter-annual subtle change in the salinity and
53 temperature (Kroon and Ganssen, 1989; Ganssen and Kroon, 1991).

54 The temperature influence on $\delta^{18}\text{O}_{ruber}$ is well defined (Mulitza et al., 2003). The effect of ambient salinity
55 on $\delta^{18}\text{O}_{ruber}$ is, however, debated (Dämmer et al., 2020). With the extensive use of $\delta^{18}\text{O}_{ruber}$ to reconstruct regional
56 evaporation-precipitation changes, especially from the monsoon dominated tropical oceans, it is imperative to
57 understand the precise influence of ambient salinity on $\delta^{18}\text{O}_{ruber}$. Additionally, the diagenetic changes, especially
58 dissolution, also substantially alters the original isotopic composition of the foraminifera shells (Berger and Killingley,
59 1977; Wu and Berger, 1989; Lohmann, 1995; McCorkle et al., 1997; Wycech et al., 2018). The studies based on the
60 comparison of ambient parameters with the isotopic composition of living specimens collected in plankton tows may
61 not address the complete range of the changes in isotopic signatures during the sinking of the tests from the surface
62 waters post death, and its subsequent deposition in the sediments at the bottom of the sea. As the fossil shells are the
63 sole basis to find out the isotopic ratio of the ambient seawater in the past, the effect of diagenetic changes including
64 the dissolution on foraminifer's oxygen isotopic ratio has to be properly evaluated. Here, we assess the influence of
65 strong salinity gradient, depth induced dissolution and other associated parameters on the stable oxygen isotopic ratio



66 of the surface dwelling planktic foraminifera *G. ruber* (white variety) in the surface sediments of the northern Indian
67 Ocean.

68

69 2. Ecology of *Globigerinoides ruber* (white)

70 *Globigerinoides ruber* is a spinose planktic foraminifera inhabiting the mixed layer waters, throughout the year, in the
71 tropical-subtropical regions (Guptha et al. 1997; Kemle-von-Mücke and Hemleben 1999). It is one of the dominant
72 planktic foraminifera in the northern Indian Ocean (Bé and Hutson, 1977; Bhadra and Saraswat, 2021) with its relative
73 abundance being as high as ~60% (Fraile et al., 2008). Its test is medium to low trochospiral and hosts algal symbionts
74 (Hemleben et al., 1989). *Globigerinoides ruber* prefers to feed upon phytoplankton (Hemleben et al., 1989), and is
75 dominant in oligotrophic warmer water with optimal temperature being 23.5°C (Fraile et al., 2008). However, it is
76 amongst a few planktic foraminifera species that can tolerate a wide range of salinity (22-49 psu) and temperature
77 (14-31°C) (Hemleben et al., 1989; Guptha et al., 1997). Two varieties of *G. ruber*, namely the white and pink are
78 common in the world oceans. However, the pink variety of *G. ruber* became extinct in the Indian and Pacific Oceans
79 at ~120 kyr during the Marine Isotopic Stage 5e (Thompson et al., 1979).

80

81 3. Northern Indian Ocean

82 The Indian Ocean with its northern boundary in the tropics includes two hydrographically contrasting basins, namely
83 the Arabian Sea and Bay of Bengal (BoB). The excess of evaporation over precipitation generates high salinity water
84 mass that spreads throughout the surface of the northern Arabian Sea with its core as deep as ~100 m (Shetye et al.,
85 1994; Prasanna Kumar and Prasad, 1999; Joseph and Freeland, 2005). Other high salinity water masses from both the
86 Persian Gulf and Red Sea enter the northern Arabian Sea at deeper depths between 200-400 m and 500-800 m,
87 respectively (Rochford, 1964). A strong upwelling along the western boundary of the Arabian Sea during the summer
88 monsoon season brings cold, nutrient rich subsurface waters to the surface (Chatterjee et al., 2019). The weak
89 upwelling during the same season is also reported in the southeastern Arabian Sea (Smitha et al., 2014).

90 The surface water is relatively fresher in the BoB, as the majority of the rivers from the Indian sub-continent
91 drain here, with the total annual continental runoff accounting to 2950 km³ (Sengupta et al., 2006). Additionally, the
92 total annual precipitation over the BoB is 4700 km³, and the evaporation is 3600 km³ (Sengupta et al., 2006). The high
93 salinity Arabian Sea water is transported into the BoB and the fresher BoB water mixes with the high salinity Arabian
94 Sea water, by the seasonally reversing coastal currents (Shankar et al., 2002). The upwelling during summer is
95 restricted to only the northwestern part of the BoB (Shetye et al., 1991). The upwelling combined with the convective
96 mixing during the winter season in the north-eastern Arabian Sea (Madhupratap et al., 1996) as well as eddies in the
97 BoB (Prasanna Kumar et al., 2004; Sarma et al., 2020) result in very high primary productivity in both basins (Qasim,
98 1977; Prasanna Kumar et al., 2009). The high primary productivity and fresh water capping induce strong stratification



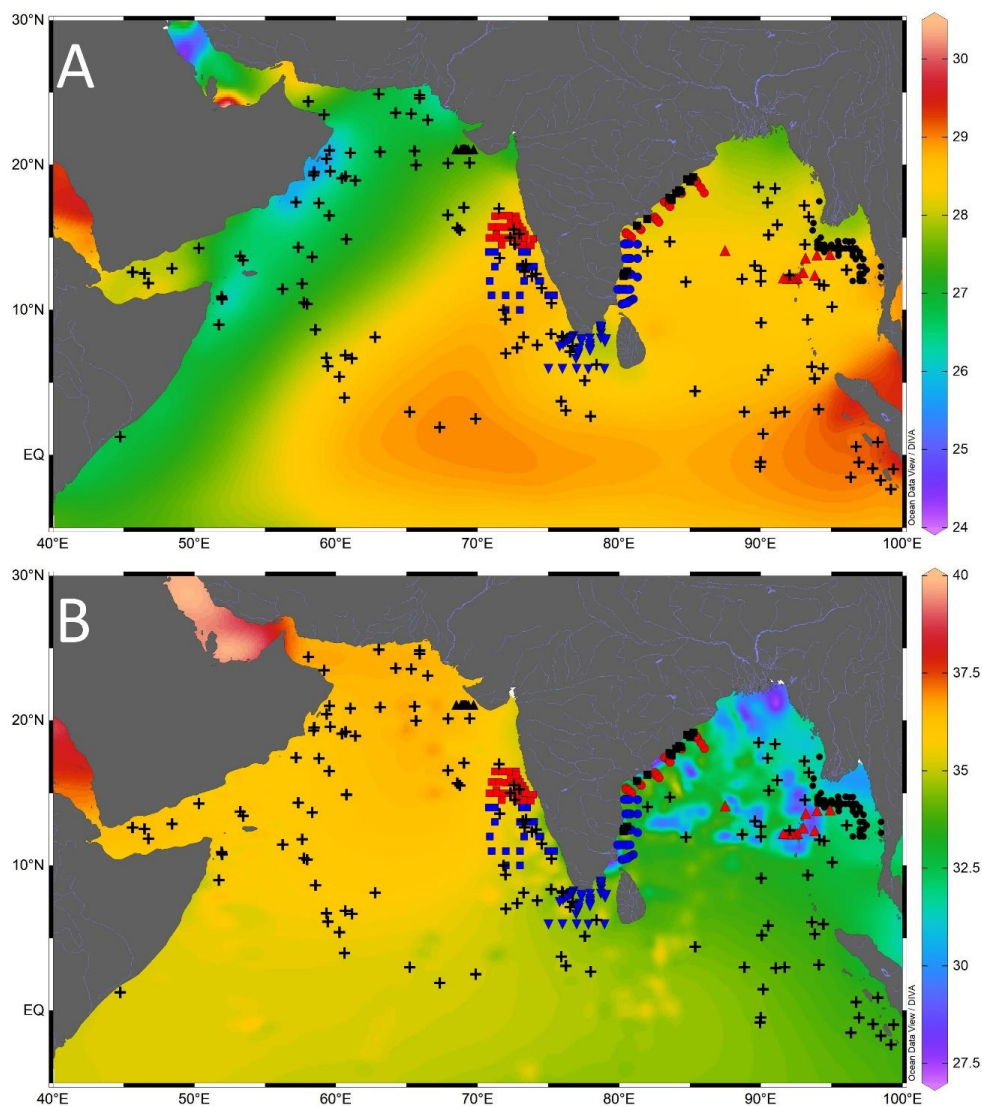
99 and restricted circulation that create oxygen deficient zones (ODZ) at the intermediate depth in both the Arabian Sea
100 (Rixen et al., 2020; Naqvi, 2021) and BoB (Bristow et al., 2016, Sridevi and Sarma, 2020). The Arabian Sea ODZ,
101 however, is comparatively thicker and intense, leading to denitrification (Naqvi et al., 2006), which is not reported yet
102 from the BoB (Bristow et al., 2016).

103 The equatorial Indian Ocean forms a part of the Indo-Pacific Warm Pool with sea surface temperature >28
104 °C throughout the year (Vinayachandran and Shetye, 1991; De Deckker, 2016). The marginal regions of the BoB are
105 comparatively warmer due to the fresh water influx from the rivers. The riverine influx shoals the mixed layer and
106 thickens the barrier layer, a buoyant layer separating the thermocline from the pycnocline, in the BoB (Howden and
107 Murtugudde, 2001). The riverine influx flows as a low salinity tongue all along the eastern margin of India (Chaitanya
108 et al., 2014). The annual average sea surface salinity (SSS) is <34 psu throughout the BoB, increasing from the head
109 bay towards south. In contrast to that, SSS remains >35 psu almost throughout the year in the Arabian Sea (Rao and
110 Sivakumar, 2003). The excess of evaporation over precipitation due to the dry northeasterly winds leads to the highest
111 salinity in the northern BoB during the winter (Rao and Sivakumar, 2003).

112

113 4. Materials and Methodology

114 Surface sediments were collected all along the path of seasonal coastal currents in the northern Indian Ocean (Figure
115 1, Supplementary Table 1). The samples from the Ayeyarwady Delta Shelf in the northeastern BoB were collected
116 during ‘India–Myanmar Joint Oceanographic Studies’ onboard Ocean Research Vessel *Sagar Kanya* (SK175). A total
117 of 110 surface sediment samples were collected from the water depths ranging from 10 m to 1080 m, on the
118 Ayeyarwady Delta Shelf (Ramaswamy et al., 2008). The multicore samples were also collected at regular intervals in
119 transects running perpendicular to the coast, from the western BoB during the cruise SK308, onboard Research Vessel
120 *Sindhu Sadhana* (cruise SSD067) and Research Vessel *Sindhu Sankalp* (cruise SSK35). A total of 84 surface samples
121 (including 71 multicore samples and 13 grab samples from sandy sediments) were collected from the inner shelf to
122 outer slope region of the eastern margin of India during the cruise SK308 (Suokhrie et al., 2021a; Saalim et al., 2022).
123 These samples from the western BoB represent the lowest salinity region in the northern Indian Ocean (Panchang and
124 Nigam, 2012). The multicore samples collected between 25 m and 2980 m in the Gulf of Mannar and the region west
125 of it (43 samples onboard Research Vessel *Sindhu Sadhana* SSD004) represent the zone of cross-basin exchange of
126 seawater between the BoB and the Arabian Sea (Singh et al., 2021). The spade core samples collected from the
127 southeastern Arabian Sea (ORV *Sagar Kanya* cruise SK117 and SK237) are located close to the distal end of the low
128 salinity BoB water intruding into the Arabian Sea. The multicore samples (13 number) collected during SSD055
129 cruise, from the northeastern Arabian Sea, represent the warm saline conditions. We also collected spade core surface
130 samples from the Andaman Sea, onboard Research Vessel *Sindhu Sankalp* (cruise SSK98). A total of 252 samples
131 had sufficient *G. ruber* for isotopic analysis. The new data was augmented with 148 previously published core-top
132 studies (e.g. Sirocko, 1989; Prell and Curry, 1981; Duplessy et al., 1981; 1982). Therefore, a total of 400 surface
133 sample data points were used for this study.



134
135

136 **Figure 1: Location of the core top samples analyzed in this study (black filled triangle - cruise SSD055, red filled square -**
137 **cruise SK117, blue filled square - cruise SK237, blue filled inverted triangle - cruise SSD004, blue filled circle - cruise**
138 **SSD067, red filled circle - cruise SK308, black filled square - cruise SSK035, red filled triangle - cruise SSK098, black filled**
139 **circle - cruise SK175) and the previously published core top values (black plus) compiled from the northern Indian Ocean.**
140 **The background contours are temperature (°C) (A) and salinity (psu) (B) with the scale on the right. Major rivers draining**
141 **into the northern Indian Ocean, are marked by blue lines.**

142 The surface sediment samples (0-1 cm) were processed following the standard procedure (Suokhrie et al., 2021b). The
143 freeze-dried sediments were weighed and wet sieved by using 63 μm sieve. The coarse fraction ($>63 \mu\text{m}$) was dry
144 sieved by using 250 μm and 355 μm sieves. For $\delta^{18}\text{O}$ analysis, 10-15 well preserved shells of *G. ruber* white variety

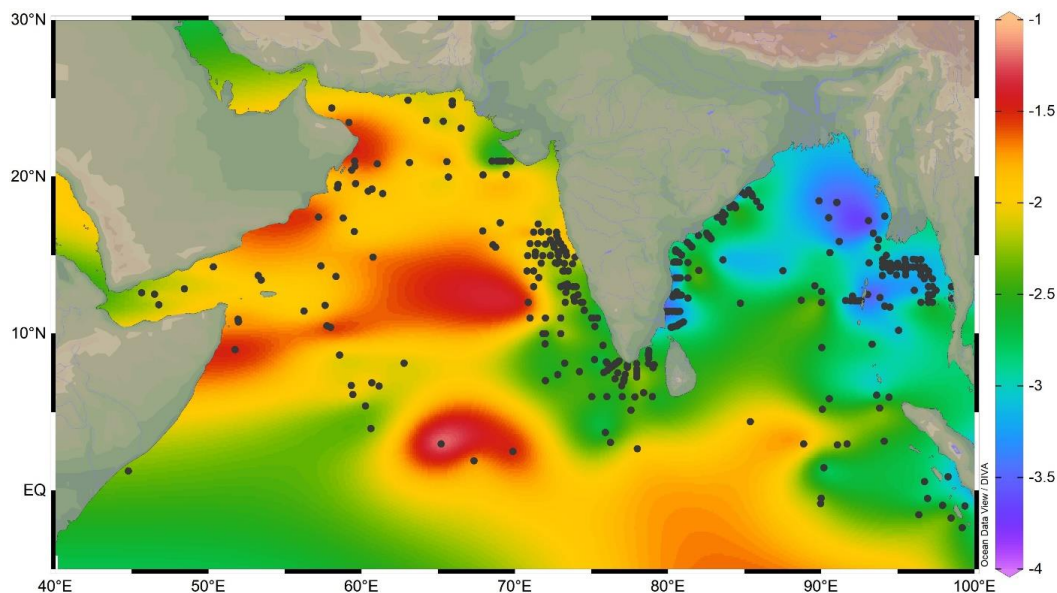


145 were picked from 250-355 μm size range. The $\delta^{18}\text{O}_{ruber}$ was measured by using Finnigan MAT 253 isotope ratio mass
146 spectrometer, coupled with Kiel IV automated carbonate preparation device. The precision of oxygen isotope
147 measurements was better than 0.08‰. The $\delta^{18}\text{O}_{ruber}$ data generated on the newly collected surface sediments was
148 augmented with the published core-top $\delta^{18}\text{O}$ measurements in the northern Indian Ocean. A total of 400 surface
149 sediment data points (252 from this work and 148 from the previous studies) were used to understand the factors
150 affecting $\delta^{18}\text{O}_{ruber}$ in the northern Indian Ocean (Supplementary Table 1). The annual average sea surface temperature
151 and salinity of the top 30 m water column at the respective sample locations was downloaded from the World Ocean
152 Atlas (Boyer et al., 2013).

153 The analyzed $\delta^{18}\text{O}_{ruber}$ data was compared with the expected $\delta^{18}\text{O}$ calcite to ascertain whether the *G. ruber*
154 properly represents the ambient conditions. For the expected $\delta^{18}\text{O}$ calcite, the $\delta^{18}\text{O}_{sw}$ was calculated from the ambient
155 salinity by using the regional seawater salinity and its stable oxygen isotopic ($\delta^{18}\text{O}_{sw}$) ratio for the entire northern
156 Indian Ocean (5°S to 30°N). The seawater salinity and corresponding $\delta^{18}\text{O}_{sw}$ data was downloaded from the Schmidt
157 et al., (1999) (version 1.22) and augmented with other regional datasets (Delaygue et al., 2001; Singh et al., 2010;
158 Achyuthan et al., 2013).
159

160 5. Results

161 The oxygen isotopic ratio of *G. ruber* varies from a minimum of -3.82‰ to the maximum of -1.09‰ in the surface
162 sediments of the northern Indian Ocean (Figure 2). The most depleted $\delta^{18}\text{O}_{ruber}$ was in the eastern BoB and the most
163 enriched values were in the western Arabian Sea.



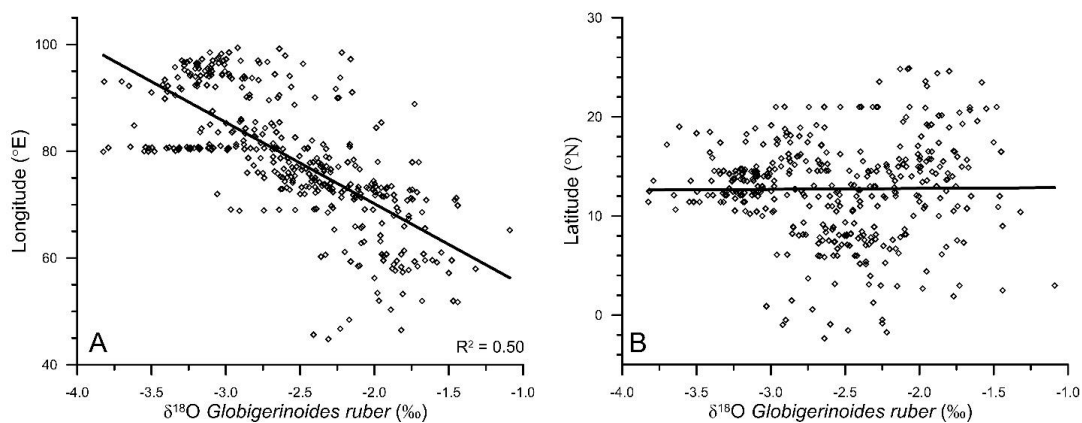
164
165
166
167
168

Figure 2: The variation in *Globigerinoides ruber* $\delta^{18}\text{O}$ (‰) in the surface sediments of the northern Indian Ocean. The stations are marked by black filled circle. The lowest $\delta^{18}\text{O}_{\text{ruber}}$ is in the riverine influx influenced northern Bay of Bengal and the highest is in the evaporation dominated central and western Arabian Sea.

169

170 The east-west gradient in $\delta^{18}\text{O}_{\text{ruber}}$ was also evident in its **significant correlation with the longitude** (Figure 3A).

171 However, $\delta^{18}\text{O}_{\text{ruber}}$ did not have any systematic latitudinal variation (Figure 3B).



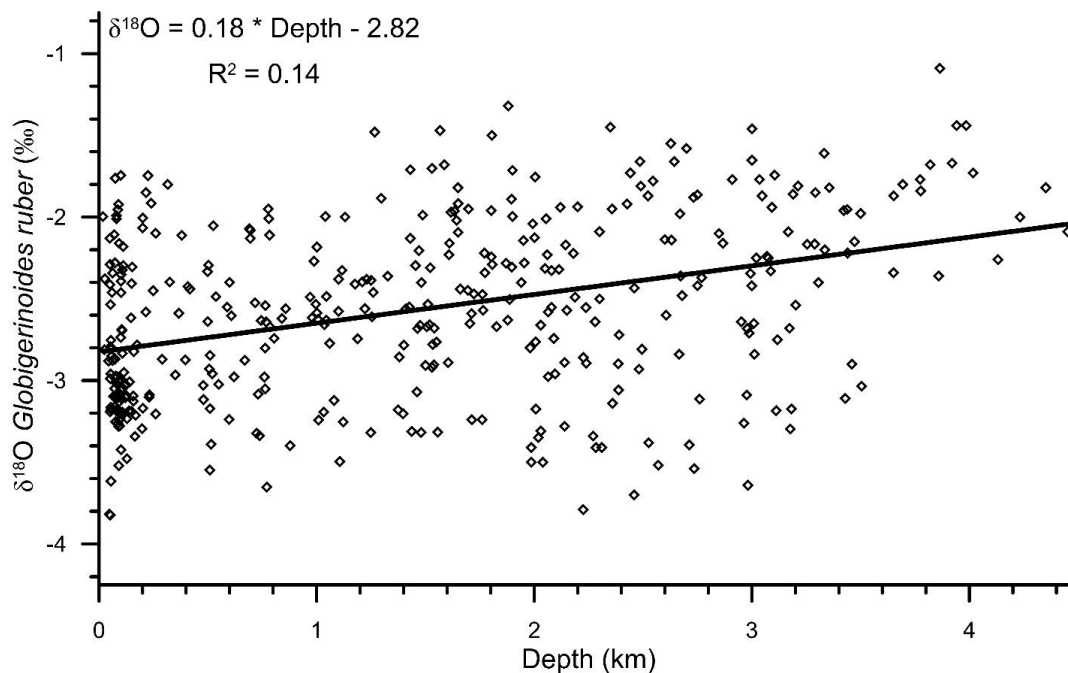
172
173
174
175

Figure 3: The variation in *Globigerinoides ruber* $\delta^{18}\text{O}$ (‰) with the corresponding longitude (A) and latitude (B), in the surface sediments of the northern Indian Ocean.

176



177 A significant correlation ($R^2 = 0.14$, $n = 400$) was observed between the water depth and $\delta^{18}\text{O}_{ruber}$ (Figure 4). $\delta^{18}\text{O}_{ruber}$
178 increased with increasing depth. The increase was gradual, without any abrupt change.

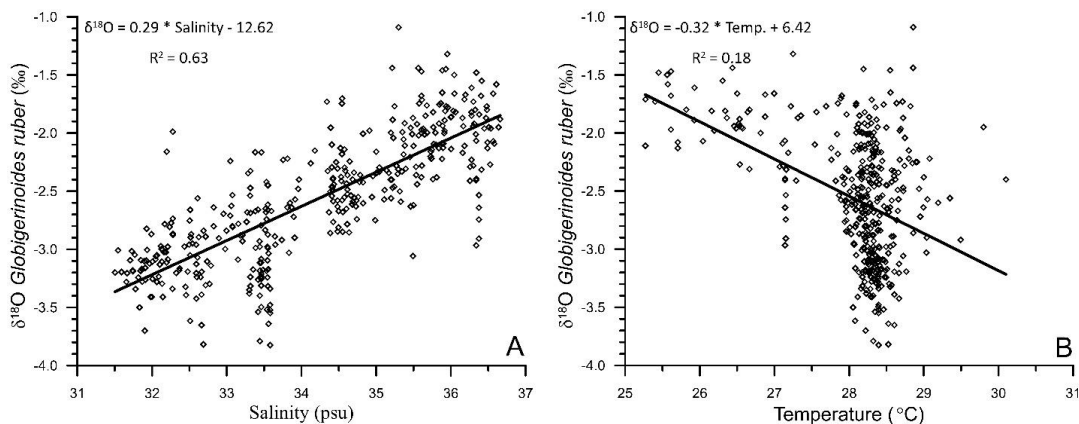


179
180

181 **Figure 4: The relationship between water depth and the oxygen isotopic ratio of mixed layer dwelling *Globigerinoides ruber*.**
182 **The trendline signifies relative enrichment of dead $\delta^{18}\text{O}_{ruber}$ shells in surface sediments, with increasing water depth.**

183

184 The uncorrected $\delta^{18}\text{O}_{ruber}$ was significantly correlated ($R^2 = 0.63$, $n = 400$) with the ambient salinity (Figure 5A).
185 However, the relationship between uncorrected $\delta^{18}\text{O}_{ruber}$ and ambient temperature was not as robust ($R^2 = 0.18$, $n =$
186 400) (Figure 5B).



187
188

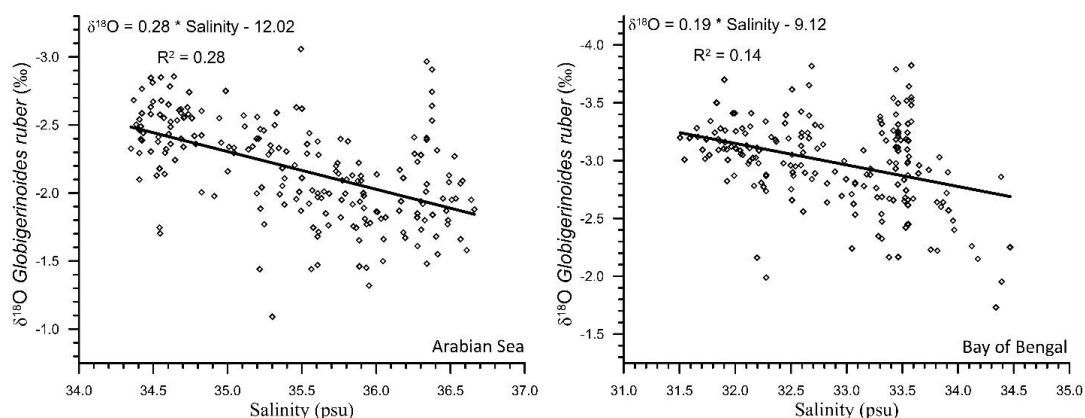


189 **Figure 5: The relationship between stable oxygen isotopic ratio of mixed layer dwelling *Globigerinoides ruber* and annual**
190 **average mixed layer salinity (A) and temperature (B) in the northern Indian Ocean.**

191

192 As the northern Indian Ocean includes two contrastingly different basins, $\delta^{18}\text{O}_{ruber}$ -salinity relationship was explored
193 for both the Arabian Sea and the BoB. A significant $\delta^{18}\text{O}_{ruber}$ -salinity relationship was observed for both the Arabian
194 Sea ($R^2 = 0.28$, $n = 205$) and BoB ($R^2 = 0.14$, $n = 195$) (Figure 6). We report a different $\delta^{18}\text{O}_{ruber}$ -salinity relationship
195 in these two basins. $\delta^{18}\text{O}_{ruber}$ increased with increasing salinity in both the BoB and the Arabian Sea.

196

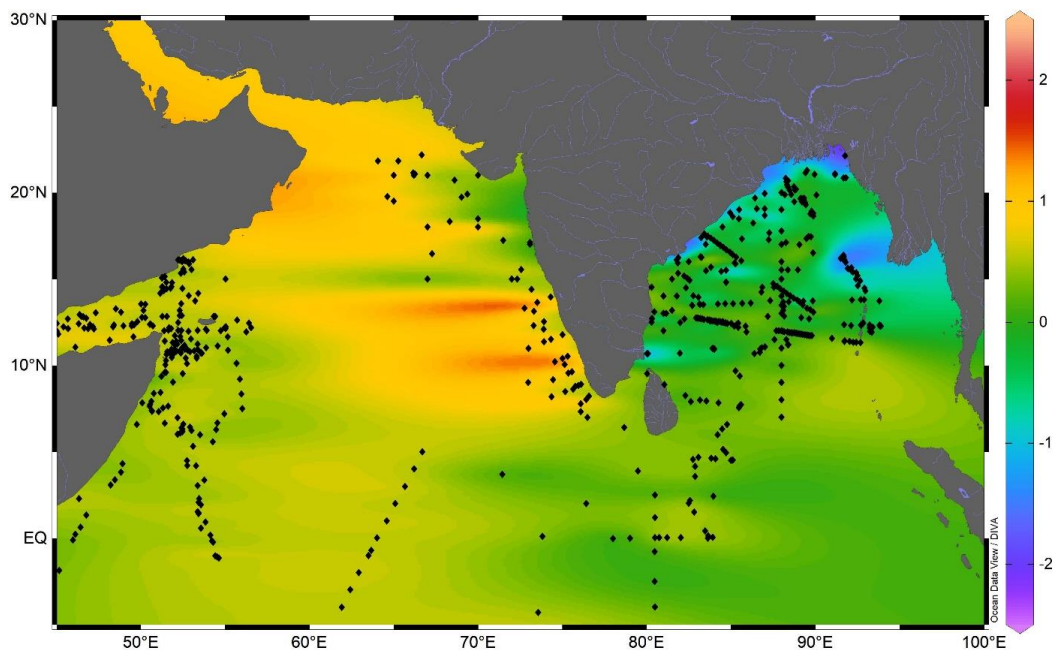


197

198 **Figure 6: The relationship between stable oxygen isotopic ratio of mixed layer dwelling *Globigerinoides ruber* and annual**
199 **average mixed layer salinity in the Arabian Sea and Bay of Bengal.**
200

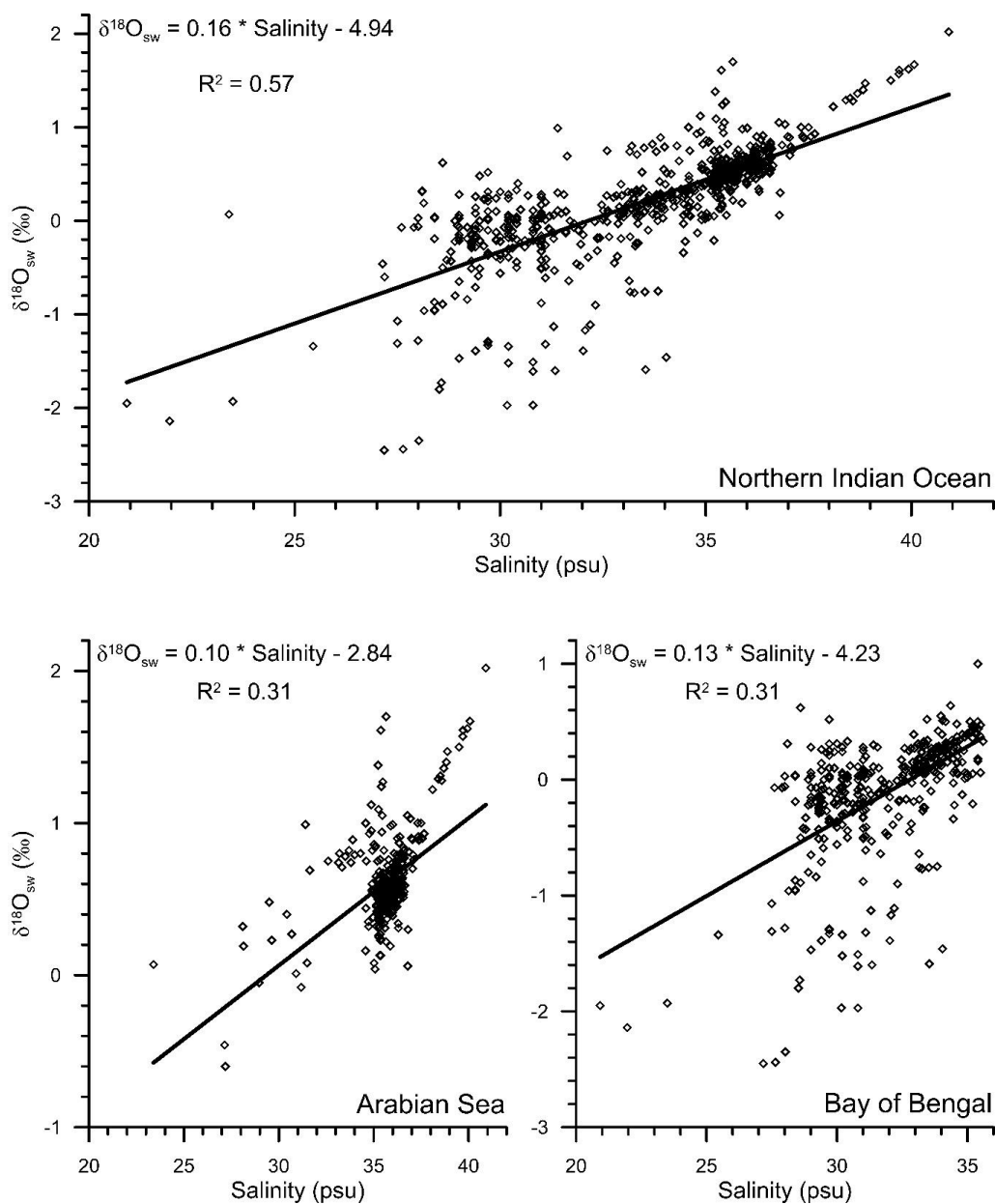
201

202 The dataset to derive the regional salinity- $\delta^{18}\text{O}_{sw}$ relationship comprises of a total of 750 stations with salinity varying
203 from 20.92 psu to 40.91 psu. The dataset also covered a large range of $\delta^{18}\text{O}_{sw}$, varying from a minimum of -2.45‰ to
204 the maximum of 2.02‰ (Figure 7, 8). **The measured $\delta^{18}\text{O}_{ruber}$ is strongly correlated ($R^2 = 0.56$, $n = 400$) with the**
205 **expected $\delta^{18}\text{O}_{calcite}$, as estimated by using the salinity- $\delta^{18}\text{O}_{sw}$ relationship and the ambient temperature.** However, the
206 relationship between seawater temperature and $\delta^{18}\text{O}_{ruber}$ - $\delta^{18}\text{O}_{sw}$, was not very robust.



207
208
209
210

Figure 7: The surface seawater oxygen isotopic ratio (‰) in the northern Indian Ocean. The black filled circles are the seawater sample locations. The thin blue lines are the major rivers draining in the northern Indian Ocean.



211
212
213

214 **Figure 8:** The relationship between surface water oxygen isotopic ratio and salinity in the northern Indian Ocean (5°S-
215 30°N), Arabian Sea and the Bay of Bengal. The data points are from Schmidt et al., (1999), Delaygue et al., (2001), Singh et
216 al., (2010), and Achyuthan et al., (2013).

217



218 6. Discussion

219 6.1 Expected versus analyzed $\delta^{18}\text{O}$

220 The estimation of expected $\delta^{18}\text{O}$ carbonate requires known seawater $\delta^{18}\text{O}$ values. The seawater $\delta^{18}\text{O}$, however, was
221 not measured. Therefore, the salinity- $\delta^{18}\text{O}_{\text{sw}}$ relationship established from the previous regional seawater isotope and
222 salinity measurements was used. The salinity- $\delta^{18}\text{O}_{\text{sw}}$ relationship varies seasonally as well as from region to region
223 (Singh et al., 2010; Achyuthan et al., 2013; Tiwari et al., 2013). Therefore, it was difficult to choose the appropriate
224 salinity- $\delta^{18}\text{O}_{\text{sw}}$ relationship. Initially, all the data points were clubbed to establish the salinity- $\delta^{18}\text{O}_{\text{sw}}$ relationship. By
225 comparing the measured $\delta^{18}\text{O}_{\text{sw}}$ with the ambient salinity, we established the following relationship for the entire
226 northern Indian Ocean (north of 5°S latitude) ($R^2 = 0.57$, $n = 750$) (Figure 8).

227

$$228 \delta^{18}\text{O}_{\text{sw}} = 0.16 * \text{Salinity} - 4.94 \quad \text{Northern Indian Ocean } (R^2 = 0.57)$$

229

230 Previously, a large difference in the slope of salinity- $\delta^{18}\text{O}_{\text{sw}}$ equation has been reported from the Arabian Sea and the
231 BoB (Delaygue et al., 2001; Singh et al., 2010; Achyuthan et al., 2013). Therefore, we also plotted the salinity- $\delta^{18}\text{O}_{\text{sw}}$
232 separately for the Arabian Sea and BoB (Figure 8). The salinity- $\delta^{18}\text{O}_{\text{sw}}$ relationship for these two basins was
233 represented by the following equations.

234

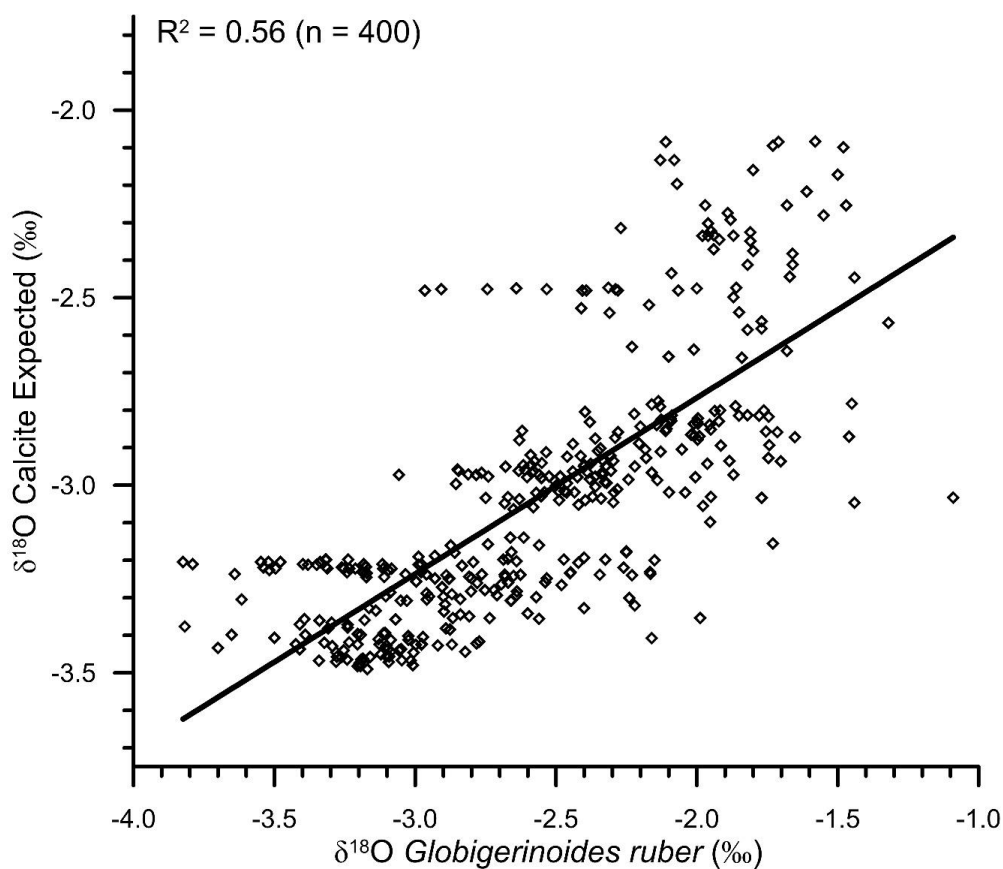
$$235 \delta^{18}\text{O}_{\text{sw}} = 0.10 * \text{Salinity} - 2.84 \quad \text{Arabian Sea} \quad (R^2 = 0.31, n = 375)$$

236

$$237 \delta^{18}\text{O}_{\text{sw}} = 0.13 * \text{Salinity} - 4.23 \quad \text{Bay of Bengal} \quad (R^2 = 0.31, n = 375)$$

238

239 The continuous flux of *G. ruber* throughout the year (Guptha et al., 1997) and the accumulation of shells in the
240 sediments over a large interval, implies that the salinity- $\delta^{18}\text{O}_{\text{sw}}$ relationship based on data representing all seasons will
241 provide a better estimate of the average $\delta^{18}\text{O}_{\text{ruber}}$ as recovered from the sediments (Vergnaud-Grazzini, 1976). The
242 expected $\delta^{18}\text{O}_{\text{sw}}$ was calculated by using these equations and the annual average mixed layer salinity at the stations
243 for which $\delta^{18}\text{O}_{\text{ruber}}$ data were available. A correction factor of 0.27‰ was applied to convert $\delta^{18}\text{O}_{\text{sw}}$ from SMOW to
244 PDB scale (Hut, 1987). The expected $\delta^{18}\text{O}$ calcite was then estimated from the calculated $\delta^{18}\text{O}_{\text{sw}}$ and the annual
245 average mixed layer temperature by using the equation proposed by Mulitza et al., (2003). We also estimated the
246 expected $\delta^{18}\text{O}$ calcite by using the low-light equation of Bemis et al (1998). The choice of equation used to estimate
247 the expected $\delta^{18}\text{O}$ calcite did not make any difference other than a constant offset. From the scatter plot (Figure 9), it
248 was clear that the analyzed $\delta^{18}\text{O}_{\text{ruber}}$ was significantly correlated ($R^2 = 0.56$, $n = 400$) with the expected $\delta^{18}\text{O}$ calcite,
249 suggesting that *G. ruber* correctly represents the ambient conditions in the entire northern Indian Ocean. The expected
250 $\delta^{18}\text{O}$ calcite estimated by using the separate Arabian Sea and BoB salinity- $\delta^{18}\text{O}_{\text{sw}}$ equations, was also similarly
251 correlated with the analyzed $\delta^{18}\text{O}_{\text{ruber}}$.



252
253
254
255
256
257

Figure 9: The scatter plot of expected $\delta^{18}\text{O}$ calcite as estimated from the ambient salinity-temperature and the analyzed $\delta^{18}\text{O}_{ruber}$. The two are significantly correlated ($R^2 = 0.63$), suggesting that *Globigerinoides ruber* correctly represents the ambient conditions.

258 6.2 Latitudinal and Longitudinal variation in $\delta^{18}\text{O}_{ruber}$

259 We report a strong ($R^2 = 0.50$) longitudinal influence on $\delta^{18}\text{O}_{ruber}$. A similar relationship with the latitudes is missing.
260 The strong longitudinal signature in $\delta^{18}\text{O}_{ruber}$ is attributed to the large salinity gradient. The huge fresh water influx in
261 the BoB reduces the SSS in the eastern Indian Ocean. The lack of major rivers in the western Arabian Sea results in
262 strong low to high salinity gradient from east to west. Although the equatorial and nearby regions are a part of the
263 Indo-Pacific Warm Pool, the limited temperature variability is evident in the insignificant latitudinal influence on
264 $\delta^{18}\text{O}_{ruber}$.

265

266 6.3 Diagenetic alteration



267 We found a strong diagenetic overprinting of $\delta^{18}\text{O}_{ruber}$ in the northern Indian Ocean (Figure 4). The enrichment of
268 $\delta^{18}\text{O}_{ruber}$ with increasing water depth suggests either dissolution leading to the preferential removal of chambers with
269 higher fraction of the lighter oxygen isotope (Wycech et al., 2018), or secondary calcification under comparatively
270 colder water (Lohmann, 1995; Schrag et al., 1995). The increase in planktic foraminifera $\delta^{18}\text{O}$ with increasing depth
271 is a common diagenetic alteration throughout the world oceans (Bonneau et al., 1980). Interestingly, the extent of the
272 increase in $\delta^{18}\text{O}_{ruber}$ with depth in the northern Indian Ocean is much smaller (0.18‰ per thousand meters) than that
273 reported for the same species from the Pacific Ocean (0.4‰ per thousand meters) (Bonneau et al., 1980). However,
274 the increase in $\delta^{18}\text{O}_{ruber}$ with depth in the northern Indian Ocean is continuous, unlike the abrupt shift in $\delta^{18}\text{O}$ (0.3-
275 0.4‰, between the depths above and below the lysocline) of another surface dwelling planktic species, namely
276 *Trilobatus sacculifer*, as observed in the western equatorial Pacific (Wu and Berger, 1989). The smaller increase in
277 $\delta^{18}\text{O}_{ruber}$ with depth is attributed to the shallower habitat of *G. ruber* as compared to *T. sacculifer*. The chamber
278 formation at different water depths implies increased heterogeneity in the *T. sacculifer* shells, with those formed at
279 warmer surface temperature being more susceptible to dissolution as compared to those formed at deeper depths during
280 the gametogenesis phase (Wycech et al., 2018). The chambers in *G. ruber* are formed at a similar depth and therefore,
281 the increase in $\delta^{18}\text{O}_{ruber}$ is continuous, while those of *T. sacculifer* are precipitated at different depths and therefore the
282 shift in $\delta^{18}\text{O}$ after a particular depth. The increase in $\delta^{18}\text{O}_{ruber}$ with depth is mainly due to the partial dissolution of the
283 more porous and thinner parts of the shells secreted at warmer temperature, as such parts are comparatively more
284 susceptible to dissolution (Berger, 1971). The increase in $\delta^{18}\text{O}_{ruber}$ with depth is similar in both the Arabian Sea and
285 BoB.

286

287 **6.4 Salinity contribution to $\delta^{18}\text{O}_{ruber}$**

288 We report a strong influence of salinity on $\delta^{18}\text{O}_{ruber}$ ($R^2=0.63$). As expected, $\delta^{18}\text{O}_{ruber}$ has a direct positive relationship
289 with the ambient salinity. The $\delta^{18}\text{O}_{ruber}$ increased by 0.29‰ for every psu increase in salinity. The northern Indian
290 Ocean has a large salinity gradient (~10 psu) from the lowest in the northern BoB to the highest in the northwestern
291 Arabian Sea. The river water and direct precipitation is enriched in the lighter isotope (Kumar et al., 2010; Kathayat
292 et al., 2021). Thus, the increased riverine influx and precipitation contributes isotopically lighter water to the surface
293 ocean (Rai et al., 2021) and decreases the $\delta^{18}\text{O}_{ruber}$. From the surface seawater samples collected during the winter
294 monsoon season (January-February 1994), a $\delta^{18}\text{O}$ -salinity slope of 0.26‰ was deduced for the Arabian Sea and of
295 0.18‰ for the BoB (Delaygue et al., 2001). However, the $\delta^{18}\text{O}$ -salinity slope varies regionally as well as during
296 different seasons (Singh et al., 2010; Achyuthan et al., 2013). The $\delta^{18}\text{O}$ -salinity slope varied from as low as 0.10 for
297 the coastal BoB samples collected during the months of April-May to as high as 0.51 for the samples collected from
298 the western BoB during the peak south-west monsoon season (August-September 1988) (Singh et al., 2010). The large
299 seasonal variation implies limitations of $\delta^{18}\text{O}$ -salinity slope deduced from snapshot surface seawater samples.
300 Additionally, *G. ruber* flux is reported throughout the year (Guptha et al., 1997), suggesting that the fossil population
301 represents annual average conditions (Thirumalai et al., 2014).



302 A different $\delta^{18}\text{O}_{ruber}$ -salinity slope for the Arabian Sea (0.28) and Bay of Bengal (0.19) is attributed to the
303 different hydrographic regimes of these two basins. The runoff and precipitation excess in the BoB results in a
304 comparatively lower salinity as compared to the evaporation dominated Arabian Sea. However, it should be noted
305 here that the relationship between $\delta^{18}\text{O}_{ruber}$ and salinity was very robust for all the northern Indian Ocean samples
306 plotted together. Interestingly, the slope of $\delta^{18}\text{O}$ -salinity for the entire northern Indian Ocean samples is much lower
307 than that for the Atlantic Ocean (0.59 for North Atlantic and 0.52 for South Atlantic, Delaygue et al., 2000) despite
308 the large meltwater influx into the north Atlantic. The difference in $\delta^{18}\text{O}$ -salinity slope despite of the huge fresh water
309 input into both the basins is because a large fraction of the riverine fresh water spreads across the surface of the
310 northern Indian Ocean, while the melt water sinks to deeper depths in the North Atlantic Ocean. A consistent
311 systematic difference has previously been observed between planktic foraminiferal shells collected in plankton tows
312 and surface sediments, with shells from the sediments being comparatively enriched in ^{18}O (Vergnaud-Grazzini,
313 1976).

314

315 **6.5 Temperature control on $\delta^{18}\text{O}_{ruber}$**

316 A first order comparison of the uncorrected $\delta^{18}\text{O}_{ruber}$ with ambient temperature of the top 30 m of the water column at
317 respective stations showed 0.32‰ decrease with every 1°C warming. The change in $\delta^{18}\text{O}_{ruber}$ as inferred from the
318 core-top sediments of the northern Indian Ocean is higher than that estimated from the plankton tows (0.22‰ per 1°C
319 change in temperature) (Mulitza et al., 2003). The seawater temperature was amongst the primary factors identified
320 to affect $\delta^{18}\text{O}_{ruber}$ (Emiliani, 1954; Mulitza et al., 2003). The low correlation between $\delta^{18}\text{O}_{ruber}$ and temperature in this
321 dataset is attributed to the limited temperature variability (1°C, 28-29°C) at a majority of the stations. The large salinity
322 difference (~6.5 psu) between stations further obscures any significant correlation between uncorrected $\delta^{18}\text{O}_{ruber}$ and
323 temperature. The temperature influence on $\delta^{18}\text{O}_{ruber}$ was thus assessed by comparing the ambient temperature with the
324 $\delta^{18}\text{O}_{ruber}$ corrected for $\delta^{18}\text{O}_{sw}$ ($\delta^{18}\text{O}_{ruber} - \delta^{18}\text{O}_{sw}$). The pH of the seawater has also been identified as a factor affecting
325 the stable oxygen isotopic composition of planktic foraminifera (Bijma et al., 1999). However, as argued by Mulitza
326 et al., (2003), the limited modern surface seawater pH variability (Chakraborty et al., 2021) and its close dependence
327 on temperature implies that the pH contribution to $\delta^{18}\text{O}_{ruber}$ is well within the error associated with the measurements.

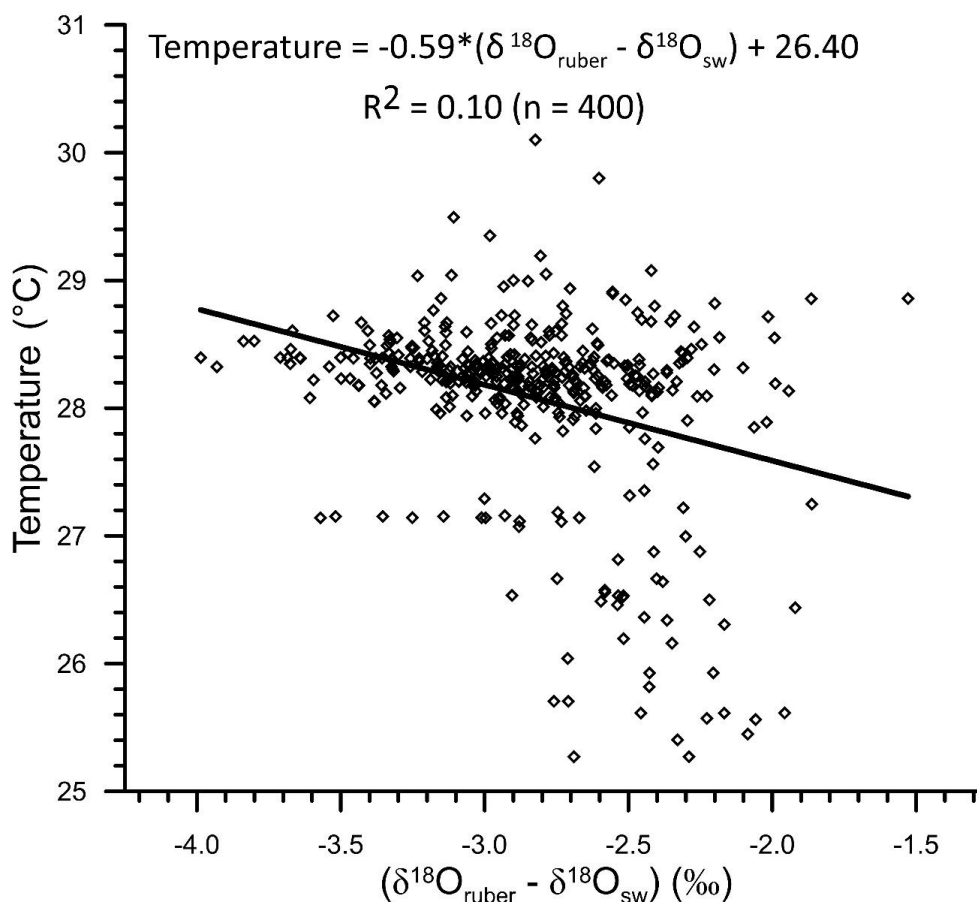
328 The comparison of $\delta^{18}\text{O}_{sw}$ corrected $\delta^{18}\text{O}_{ruber}$ with the ambient temperature also confirms the enrichment of
329 ($\delta^{18}\text{O}_{ruber} - \delta^{18}\text{O}_{sw}$) in heavier oxygen isotope with the decrease in temperature (Figure 10). We obtained the following
330 relationship between temperature and ($\delta^{18}\text{O}_{ruber} - \delta^{18}\text{O}_{sw}$) in the northern Indian Ocean.

331

$$332 \text{ Temperature} = -0.59 * (\delta^{18}\text{O}_{ruber} - \delta^{18}\text{O}_{sw}) + 26.40$$

333

334 The slope of the temperature and ($\delta^{18}\text{O}_{ruber} - \delta^{18}\text{O}_{sw}$) was somewhat different (0.17‰ per 1°C change in temperature)
335 than that of the temperature versus uncorrected $\delta^{18}\text{O}_{ruber}$, but similar as that reported for the plankton tows (0.22‰ per
336 1°C change in temperature) (Mulitza et al., 2003).



337
338

339 **Figure 10: The relationship between ambient temperature and $(\delta^{18}\text{O}_{\text{ruber}} - \delta^{18}\text{O}_{\text{sw}})$ for the northern Indian Ocean. As**
340 **expected the $(\delta^{18}\text{O}_{\text{ruber}} - \delta^{18}\text{O}_{\text{sw}})$ gets enriched in heavier isotope with decreasing ambient temperature.**

341

342 7. Conclusions

343 We measured the stable oxygen isotopic ratio of the surface dwelling planktic foraminifera *Globigeroide*
344 white variety from the surface sediments of the northern Indian Ocean. A comparison of the $\delta^{18}\text{O}_{\text{ruber}}$ with the depth
345 suggests a strong diagenetic alteration of the isotopic ratio. The ambient salinity exerts the maximum influence on the
346 $\delta^{18}\text{O}_{\text{ruber}}$ suggesting its robust application to reconstruct past salinity in the northern Indian Ocean. The large east-west
347 salinity gradient in the northern Indian Ocean results in a strong longitudinal variation in $\delta^{18}\text{O}_{\text{ruber}}$. The temperature
348 influence on $\delta^{18}\text{O}_{\text{ruber}}$ is subdued as compared to the effect of large salinity variation in the northern Indian Ocean. We



349 report a relatively smaller change in $\delta^{18}O_{ruber}$ with a unit increase in ambient temperature in case of specimens retrieved
350 from the surface sediments as compared to those collected live from the water column.

351 **8. Data Availability**

352 The newly generated data as well as the data compiled from previous studies from the northern Indian Ocean has been
353 submitted to PANGAEA and is available at
354 <https://www.pangaea.de/tok/59190adf9e4facf7ebb9ad555c0bce58a9a72bd9> (Saraswat et al., 2022). The data is
355 submitted with the manuscript as well, for the reviewers' scrutiny.

356 **9. Author Contribution**

357 RS designed the research, compiled and interpreted the data and wrote the manuscript. TS, DKN, DPS, SMS, MS,
358 GS, SRB, SRK picked the specimens for isotopic analysis. MM, ASM supervised the analysis. All authors edited and
359 contributed to the final manuscript.

360 **10. Competing Interests**

361 The authors declare that they have no conflict of interest.

362 **Acknowledgements**

363 We thank the crew onboard expeditions during which the surface sediment samples were collected. The authors thank
364 the Director, CSIR-National Institute of Oceanography for the facilities and funding. The technical personnel at the
365 Alfred-Wegener Institute for Polar and Marine Research, and MARUM, Bremen University, Germany are
366 acknowledged for the help in stable isotopic analysis. We thank Dr. V. Ramaswamy, CSIR-NIO for providing the
367 surface sediment samples collected from the Myanmar continental shelf. The authors also thank Dr. B.N. Nath for
368 providing the spade core-top samples from the eastern margin of India.

369

370



371 **References**

372

- 373 Achyuthan, H., R.D. Deshpande, M.S. Rao, B. Kumar, T. Nallathambi, K. Shashi Kumar, R. Ramesh, P.
374 Ramachandran, A.S. Maurya, and S.K. Gupta: Stable isotopes and salinity in the surface waters of the Bay of
375 Bengal: Implications for water dynamics and palaeoclimate. *Mar. Chem.*, 149, 51-62, 2013.
- 376 Bé, A.W.H., and Hutson, W.H.: Ecology of planktonic foraminifera and biogeographic patterns of life and fossil
377 assemblages in the Indian Ocean. *Micropaleontology*, 23, 369, 1977.
- 378 Bemis, B.E., Spero, H.J., Bijma, J., and Lea, D.W.: Reevaluation of the oxygen isotopic composition of planktonic
379 foraminifera: Experimental results and revised paleotemperature equations. *Paleoceanography* 13, 150-160, 1998.
- 380 Berger, W.H., 1971. Sedimentation of planktonic foraminifera. *Mar. Geol.*, 11, 325-358.
- 381 Berger, W.H., and J.S. Killingley: Glacial-Holocene transition in deep-sea carbonates: selective dissolution and the
382 stable isotope signal. *Science*, 197, 563-566, 1977.
- 383 Bhadra, S.R., and R. Saraswat: Assessing the effect of riverine discharge on planktic foraminifera: A case study from
384 the marginal marine regions of the western Bay of Bengal. *Deep Sea Res. II: Topical Stud. Oceanogra.*, 183,
385 104927, 2021.
- 386 Bijma, J., Spero, H.J., and Lea, D.W.: Reassessing foraminiferal stable isotope geochemistry: Impact of the oceanic
387 carbonate system (experimental results). In: Fischer, G., Wefer, G. (Eds.), *Use of Proxies in Paleoceanography:
388 Examples from the South Atlantic*. Springer, Berlin, pp. 489-512, 1999.
- 389 Bonneau, M.-C., C. Vergnaud-Grazzini, and W.H. Berger: Stable isotope fractionation and differential dissolution in
390 Recent planktonic foraminifera from Pacific box-cores. *Oceanologica Acta*, 3, 377-382, 1980.
- 391 Boyer, T. P., Antonov, J. I., Baranova, O. K., Garcia, H. E., Johnson, D. R., Mishonov, A. V., et al.: *World Ocean
392 Database*, 2013.
- 393 Bristow, L.A., C.M Callbeck, M. Larsen, M.A. Altabet, J. Dekaezemacker, M. Forth, M. Gauns, R.N. Glud, M.M.M.
394 Kuypers, G. Lavik, J. Milucka, S.W. A. Naqvi, A. Pratihary, N. P. Revsbech, B. Thamdrup, A. H. Treusch, and D.
395 E. Canfield: N₂ production rates limited by nitrite availability in the Bay of Bengal oxygen minimum zone. *Nat.
396 Geosci.*, 10, 24-29, 2017.
- 397 Chaitanya, A.V.S., M. Lengaigne, J. Vialard, V.V. Gopalakrishna, F. Durand, C. Kranthikumar, S. Amritash, V.
398 Suneel, F. Papa, and M. Ravichandran: Salinity measurements collected by fishermen reveal a “river in the sea”
399 flowing along the eastern coast of India. *Bull. American Met. Soc.*, 95, 1897-1908, 2014.
- 400 Chakraborty, K., V. Valsala, T. Bhattacharya, and J. Ghosh: Seasonal cycle of surface ocean pCO₂ and pH in the
401 northern Indian Ocean and their controlling factors. *Progr. Oceanogra.*, 198, 102683, 2021.
- 402 Chatterjee, A., B.P. Kumar, S. Prakash, and P. Singh: Annihilation of the Somali upwelling system during summer
403 monsoon. *Sci. Rep.*, 9, 1-14, 2019.
- 404 Dämmer, L.K., L. de Nooijer, E. van Sebille, J.G. Haak, and G.-J. Reichert: Evaluation of oxygen isotopes and trace
405 elements in planktonic foraminifera from the Mediterranean Sea as recorders of seawater oxygen isotopes and
406 salinity. *Clim. Past*, 16, 2401-2414, 2020.



- 407 De Deckker, P.: The Indo-Pacific Warm Pool: critical to world oceanography and world climate. *Geosci. Lett.*, 3, 20,
408 2016.
- 409 Delaygue, G., E. Bard, C. Rollion, J. Jouzel, M. Stievenard, and J.-C. Duplessy: Oxygen isotope/salinity relationship
410 in the northern Indian Ocean. *J. Geophys. Res.*, 106, 4565-4574, 2001.
- 411 Delaygue, G., J. Jouzel, and J.C. Dutay: Oxygen 18–salinity relationship simulated by an oceanic general circulation
412 model. *Earth Planet. Sci. Lett.*, 178, 113-123, 2000.
- 413 Duplessy, J.C., Bé, A.W.H., and Blanc, P.L.: Oxygen and carbon isotopic composition and biogeographic distribution
414 of planktonic foraminifera in the Indian Ocean. *Palaeogeogra., Palaeoclimatol., Palaeoecol.*, 33, 9-46, 1981.
- 415 Duplessy, J.C.: Glacial to interglacial contrasts in the northern Indian Ocean. *Nature*, 295, 494-498, 1982.
- 416 Duplessy, J.C., Blanc, P.L., and Bé, A.W.H.: Oxygen-18 enrichment of planktonic foraminifera due to gametogenic
417 calcification below the euphotic zone. *Science*. 213, 1247-1250, 1981.
- 418 Emiliani, C.: Depth habitat of some species of pelagic foraminifera as indicated by oxygen isotope ratio. *American J.*
419 *Sci.*, 252, 149-158, 1954.
- 420 Erez, J., Luz, B.: Experimental paleotemperature equation for planktonic foraminifera. *Geochim. Cosmochim. Acta*,
421 47, 1025-1031, 1983.
- 422 Fraile, I., M. Schulz, S. Mulitza, and M. Kucera: Predicting the global distribution of planktonic foraminifera using a
423 dynamic ecosystem model. *Biogeosciences*, 5, 891-911, 2008.
- 424 Ganssen, G., and Kroon, D.: Evidence for Red Sea surface water circulation from oxygen isotopes of modern surface
425 waters and planktonic foraminiferal tests. *Paleoceanography*, 6, 73-82, 1991.
- 426 Gupta, M.V.S., Curry, W.B., Ittekkot, V., and Muralinath, A.S.: Seasonal variation in the flux of planktic
427 foraminifera: Sediment trap results from the Bay of Bengal, northern Indian Ocean. *J. Foraminiferal Res.*, 27, 5-
428 19, 1997.
- 429 Hemleben, C., Spindler, M., and Anderson, O. R.: *Modern Planktonic Foraminifera*, Springer-Verlag, New York,
430 1989.
- 431 Hollstein, M., Mohtadi, M., Rosenthal, Y., Moffa Sanchez, P., Oppo, D., Martínez Méndez, G., Steinke, S., and
432 Hebbeln, D.: Stable oxygen isotopes and Mg/Ca in planktic foraminifera from modern surface sediments of the
433 Western Pacific Warm Pool: Implications for thermocline reconstructions. *Paleoceanography*, 32, 1174-1194,
434 2017.
- 435 Horikawa, K., T. Kodaira, J. Zhang, and M. Murayama: $\delta^{18}\text{O}_{\text{sw}}$ estimate for *Globigerinoides ruber* from core-top
436 sediments in the East China Sea. *Progr. Earth Planet. Sci.*, 2, 19, 2015.
- 437 Howden, S. D., and Murtugudde, R.: Effects of river inputs into the Bay of Bengal. *J. Geophys. Res.*, 106(C9), 19825-
438 19844, 2001.
- 439 Hut, G.: Consultants group meeting on stable isotope reference samples for geochemical and hydrological
440 investigations. Report to the Director General, International Atomic Energy Agency, Vienna, 42 pp, 1987.
- 441 Joseph, S., and Freeland, H.J.: Salinity variability in the Arabian Sea. *Geophysical Research Letters*, 32, L09607,
442 2005.



- 443 Kathayat, G., Sinha, A., Tanoue, M., K. Yoshimura, H. Li, Zhang, H., and Cheng, H.: Interannual oxygen isotope
444 variability in Indian summer monsoon precipitation reflects changes in moisture sources. *Communication Earth*
445 *Environ.*, 2, 96, 2021.
- 446 Kemle-von-Mücke, S., and Hemleben, C.: Planktic Foraminifera. In: Boltovskoy E (ed) South Atlantic zooplankton.
447 Backhuys Publishers, Leiden, pp 43-67, 1999.
- 448 Kessarkar, P.M., Purnachadra Rao, V., Naqvi, S.W.A., and Karapurkar, S.G.: Variation in the Indian summer monsoon
449 intensity during the Bølling-Ållerød and Holocene. *Paleoceanography*, 28, 413-425, 2013.
- 450 Kim, S.T., and O'Neil, J.R.: Equilibrium and nonequilibrium oxygen isotope effects in synthetic carbonates.
451 *Geochimica Cosmochim Acta*, 61, 3461-3475, 1997.
- 452 Kroon, D., and Ganssen, G.: Northern Indian Ocean upwelling cells and the stable isotope composition of living
453 planktonic foraminifers. *Deep-Sea Res.*, 36, 1219-1236, 1989.
- 454 Kumar, B., S. P. Rai, U. Saravana Kumar, S. K. Verma, P. Garg, S. V. Vijaya Kumar, R. Jaiswal, B. K. Purendra, S.
455 R. Kumar, and N.G. Pande: Isotopic characteristics of Indian precipitation. *Water Resource Res.*, 46, W12548,
456 2010.
- 457 Lambeck, K., H. Rouby, A. Purcell, Y. Sun, and M. Sambridge: Sea level and global ice volumes from the Last Glacial
458 Maximum to the Holocene. *Proc. Nat. Acad. Sci.*, 111, 15296–15303, 2014.
- 459 Lea, D.W.: Elemental and isotopic proxies of past ocean temperatures. *Treatise Geochem.*, 8, 373-397, 2014.
- 460 Lohmann, G. P.: A model for variation in the chemistry of planktonic foraminifera due to secondary calcification and
461 selective dissolution. *Paleoceanography*, 10, 445-457, 1995.
- 462 Madhupratap, M., S.P. Kumar, P.M.A. Bhattathiri, M.D. Kumar, S. Raghukumar, K.K.C. Nair, and N. Ramaiah:
463 Mechanism of the biological response to winter cooling in the northeastern Arabian Sea. *Nature*, 384, 549-552,
464 1996.
- 465 Mahesh, B.S., and Banakar, V.K.: Change in the intensity of low-salinity water inflow from the Bay of Bengal into
466 the Eastern Arabian Sea from the Last Glacial Maximum to the Holocene: Implications for monsoon variations.
467 *Palaeogeogra., Palaeoclimatol., Palaeoecol.*, 397, 31-37, 2014.
- 468 McCorkle, D. C., Martin, P. A., Lea, D. W., and Klinkhammer, G.P.: Evidence of a dissolution effect on benthic
469 foraminiferal shell chemistry: $\delta^{13}\text{C}$, Cd/Ca, Ba/Ca, and Sr/Ca results from the Ontong Java Plateau.
470 *Paleoceanography*, 10, 699-714, 1997.
- 471 Metcalfe, B., Feldmeijer, W., and Ganssen, G.M.: Oxygen isotope variability of planktonic foraminifera provide clues
472 to past upper ocean seasonal variability. *Paleoceanogra. Paleoclimatol.*, 34, 374–393, 2019.
- 473 Mohtadi, M., Oppo, D.W., Lückge, A., DePol-Holz, R., Steinke, S., Groeneveld, J., Hemme, N., and Hebbeln, D.:
474 Reconstructing the thermal structure of the upper ocean: Insights from planktic foraminifera shell chemistry and
475 alkenones in modern sediments of the tropical eastern Indian Ocean. *Paleoceanography*, 26, PA3219, 2011.
- 476 Mulitza, S., Boltovskoy, D., Donner, B., Meggers, H., Paul, A., and Wefer, G.: Temperature: $\delta^{18}\text{O}$ relationships of
477 planktonic foraminifera collected from surface waters. *Palaeogeogra., Palaeoclimatol., Palaeoecol.*, 202, 143-152,
478 2003.



- 479 Mulitza, S., Dürkoop, A., Hale, W., Wefer, G., and Niebler, H.S.: Planktonic foraminifera as recorders of past surface-
480 water stratification. *Geology*, 25, 335-338, 1997.
- 481 Mulitza, S., Wolff, T., Pätzold, J., Hale, W., and Wefer, G.: Temperature sensitivity of planktic foraminifera and its
482 influence on the oxygen isotope record. *Mar. Micropaleontol.*, 33, 223-240, 1998.
- 483 Naqvi, S.W.A.: Deoxygenation in marginal seas of the Indian Ocean. *Front. Mar. Sci.*, 8, 624322. doi:
484 10.3389/fmars.2021.624322, 2021.
- 485 Naqvi, S.W.A., H. Naik, A. Pratihary, W. D'souza, P.V. Narvekar, D.A. Jayakumar, A.H. Devol, T. Yoshinari, and T.
486 Saino: Coastal versus open-ocean denitrification in the Arabian Sea. *Biogeosciences*, 3, 621-633, 2006.
- 487 Panchang, R., and Nigam, R.: High resolution climatic records of the past~ 489 years from Central Asia as derived
488 from benthic foraminiferal species, *Asterorotalia trispinosa*. *Mar. Geol.*, 307, 88-104, 2012.
- 489 Pearson, P.N.: Oxygen isotopes in foraminifera: Overview and historical review. In *Reconstructing Earth's Deep-*
490 *Time Climate—The State of the Art in 2012*, Paleontological Society Short Course, November 3, 2012. The
491 Paleontological Society Papers, Volume 18, Linda C. Ivany and Brian T. Huber (eds.), pp. 1-38, 2012.
- 492 Prasanna Kumar, S., J. Narvekar, M. Nuncio, M. Gauns, and S. Sardesai: What drives the biological productivity of
493 the northern Indian Ocean? Washington DC American Geophysical Union Geophysical Monograph Series, 185,
494 33-56, 2009.
- 495 Prasanna Kumar, S., M. Nuncio, J. Narvekar, A. Kumar, D.S. Sardesai, S.N. De Souza, M. Gauns, N. Ramaiah, and
496 M. Madhupratap: Are eddies nature's trigger to enhance biological productivity in the Bay of Bengal? *Geophys.*
497 *Res. Lett.*, 31, L07309, doi:10.1029/2003GL019274, 2004.
- 498 Prasanna Kumar, S., and Prasad, T.G.: Formation and spreading of Arabian Sea high-salinity water mass. *J. Geophys.*
499 *Res: Oceans*, 104, 1455-1464, 1999.
- 500 Prell, W.L., Curry, W.B.: Faunal and isotopic indices of monsoonal upwelling: Western Arabian Sea. *Oceanologica*
501 *Acta*, 4, 91-98, 1981.
- 502 Qasim, S.Z.: Biological productivity of the Indian Ocean. *Indian J. Mar. Sci.*, 6, 122-137, 1977.
- 503 Rai, S.P., J. Noble, D. Singh, Y.S. Rawat, and B. Kumar: Spatiotemporal variability in stable isotopes of the Ganga
504 River and factors affecting their distributions. *Catena*, 204, 105360, 2021.
- 505 Ramaswamy, V., Gaye, B., Shirodkar, P.V., Rao, P.S., Chivas, A. R., Wheeler, D., and Thwin, S.: Distribution and
506 sources of organic carbon, nitrogen and their isotopic signatures in sediments from the Ayeyarwady (Irrawaddy)
507 continental shelf, northern Andaman Sea. *Mar. Chem.*, 111, 137-150, 2008.
- 508 Rao, R. R., and Sivakumar, R.: Seasonal variability of sea surface salinity and salt budget of the mixed layer of the
509 northIndian Ocean. *J. Geophys. Res.*, 108(C1), 3009, 2003.
- 510 Rixen, T., G. Cowie, B. Gaye, J. Goes, H. do Rosário Gomes, R.R. Hood, Z. Lachkar, H. Schmidt, J. Segschneider,
511 and A. Singh: Reviews and syntheses: Present, past, and future of the oxygen minimum zone in the northern Indian
512 Ocean. *Biogeosciences*, 17, 6051-6080, 2020.
- 513 Rochford, D. J.: Salinity maximum in the upper 100 meters of the north Indian Ocean. *Aust. J. Mar. Freshwater Res.*,
514 15, 1-24, 1964.



- 515 Saalim, S.M., Saraswat, R., and Nigam, R.: Ecological preferences of living benthic foraminifera from the Mahanadi
516 river-dominated north-western Bay of Bengal: A potential environmental impact assessment tool. *Mar. Poll. Bull.*,
517 175, 113158, 2022.
- 518 Saraswat, R., Lea, D.W., Nigam, R., Mackensen, A., and Naik, D.K.: Deglaciation in the tropical Indian Ocean driven
519 by interplay between the regional monsoon and global teleconnections. *Earth Planet. Sci. Lett.*, 375, 166-175,
520 2013.
- 521 Saraswat, R., Nigam, R., Mackensen, A., and Weldeab, S.: Linkage between seasonal insolation gradient in the tropical
522 northern hemisphere and the sea surface salinity of the equatorial Indian Ocean during the last glacial period. *Acta*
523 *Geol. Sinica*, 86, 801–811, 2012.
- 524 Saraswat, R., D.P. Singh, D.W. Lea, A. Mackensen, and D.K. Naik: Indonesian throughflow controlled the westward
525 extent of the Indo-Pacific Warm Pool during glacial-interglacial intervals. *Global Planet. Cha.*, 183, 103031, 2019.
- 526 Saraswat, R., Suokhrie, T., Naik, D.K., Singh, D.P., Saalim, S.M., Salman, M., Kumar, G., Bhadra, S.R., Mohtadi,
527 M., Kurtarkar, S.R., Maurya, A.S., 2022. Oxygen isotopic ratio of *Globigerinoides ruber* (white variety) in the
528 surface sediments of the northern Indian Ocean. PANGAEA, <https://doi.org/10.1594/PANGAEA.945401>
- 529 Sarma, V.V.S.S., M. Chopra, D.N. Rao, M.M.R. Priya, G.R. Rajula, D.S.R. Lakshmi, and V.D. Rao: Role of eddies
530 on controlling total and size-fractionated primary production in the Bay of Bengal. *Cont. Shelf Res.*, 204, 104186,
531 2020.
- 532 Schmidt, G.A., Bigg, G. R., and Rohling, E.J.: "Global Seawater Oxygen-18 Database - v1.22"
533 <https://data.giss.nasa.gov/o18data/>, 1999.
- 534 Schrag, D.P., DePaolo, D.J., Richter, F.M.: Reconstructing past sea surface temperatures: Correcting for diagenesis
535 of bulk marine carbonate. *Geochim. Cosmochim. Acta*, 59, 2265–2278, 1995.
- 536 Sengupta, D., Bharath Raj, G.N., and Shenoi, S.S.C.: Surface freshwater from Bay of Bengal runoff and Indonesian
537 Throughflow in the tropical Indian Ocean. *Geophys. Res. Lett.*, 33, L22609, 2006.
- 538 Shackleton, N.J.: Oxygen isotopes, ice volume and sea level. *Quat. Sci. Rev.*, 6, 183-190, 1987.
- 539 Shackleton, N.J.: The 100,000-year Ice-Age cycle identified and found to lag temperature, carbon dioxide, and orbital
540 eccentricity. *Science*, 289, 1897-1902, 2000.
- 541 Shackleton, N.J., and Vincent, E.: Oxygen and carbon isotope studies in recent foraminifera from the southwest Indian
542 ocean. *Mar. Micropaleontol.*, 3, 1-13, 1978.
- 543 Shankar, D., Vinayachandran, P.N., and Unnikrishnan, A.S.: The monsoon currents in the north Indian Ocean. *Progr.*
544 *Oceanogra.*, 52, 63–120, 2002.
- 545 Shetye, S.R., Gouveia, A.D., and Shenoi, S.S.C.: Circulation and water masses of the Arabian Sea. *Proc. Indian Acad.*
546 *Sci. (Earth Planet. Sci.)*, 103, 107-123, 1994.
- 547 Shetye, S.R., S.S.C. Shenoi, A.D. Gouveia, G.S. Michael, D. Sundar, and G. Nampoothiri: Wind-driven coastal
548 upwelling along the western boundary of the Bay of Bengal during the southwest monsoon. *Cont. Shelf Res.*, 11,
549 1397-1408, 1991.
- 550 Singh, A., Jani, R.A., and Ramesh, R.: Spatiotemporal variations of the $\delta^{18}\text{O}$ –salinity relation in the northern Indian
551 Ocean. *Deep-Sea Res. I*, 57, 1422–1431, 2010.



- 552 Singh, D.P., Saraswat, R., and Nigam, R.: Untangling the effect of organic matter and dissolved oxygen on living
553 benthic foraminifera in the southeastern Arabian Sea. *Mar. Poll. Bull.*, 172, 112883, 2021.
- 554 Sirocko, F.: Zur Akkumulation von Staubsedimenten im nördlichen Indischen Ozean; Anzeiger der Klimageschichte
555 Arabiens und Indiens. Dissertation, Berichte-Reports, Geologisch-Paläontologisches Institut der Universität Kiel,
556 27, 185 pp, 1989.
- 557 Smitha, A., K.A. Joseph, C. Jayaram, and A.N. Balchand: Upwelling in the southeastern Arabian Sea as evidenced by
558 Ekman mass transport using wind observations from OCEANSAT–II Scatterometer. *Indian J. Geo-mar. Sci.*, 43,
559 111-116, 2014.
- 560 Spero, H.J., Bijma, J., Lea, D.W., and Bemis, B.B.: Effect of seawater carbonate concentration on foraminiferal carbon
561 and oxygen isotopes. *Nature* 390, 497-500, 1997.
- 562 Sridevi, B., and V.V.S.S. Sarma: A revisit to the regulation of oxygen minimum zone in the Bay of Bengal. *J. Earth
563 Syst. Sci.*, 129, 1-7, 2020.
- 564 Stainbank, S., Kroon, D., Rüggeberg, A., Raddatz, J., de Leau, E.S., Zhang, M., et al.: Controls on planktonic
565 foraminifera apparent calcification depths for the northern equatorial Indian Ocean. *PLoS ONE* 14(9), e0222299,
566 2019.
- 567 Suokhrie, T., Saraswat, R., Nigam, R.: Multiple ecological parameters affect living benthic foraminifera in the river-
568 influenced west-central Bay of Bengal. *Front. Mar. Sci.*, 8, 467, 2021a.
- 569 Suokhrie, T., Saraswat, and R., Saju, S.: Strong solar influence on multi-decadal periodic productivity changes in the
570 central-western Bay of Bengal. *Quat. Int.*, <https://doi.org/10.1016/j.quaint.2021.04.015>, 2021b.
- 571 Thirumalai, K., Richey, J.N., Quinn, T.M., and Poore, R.Z.: *Globigerinoides ruber* morphotypes in the Gulf of
572 Mexico: A test of null hypothesis. *Sci. Rep.*, 4, 6018, 2014.
- 573 Thompson, P.R., Bé, A.W.H., Duplessy, J.-C., and Shackleton, N.J.: Disappearance of pink-pigmented
574 *Globigerinoides ruber* at 120,000 yr BP in the Indian and Pacific oceans. *Nature*, 280, 554-558, 1979.
- 575 Tiwari, M., Nagoji, S.S., Kartik, T., Drishya, G., Parvathy, R.K., and Rajan, S.: Oxygen isotope–salinity relationships
576 of discrete oceanic regions from India to Antarctica vis-à-vis surface hydrological processes. *J. Mar. Syst.*, 113-
577 114, 88-93, 2013.
- 578 Urey, H. C.: The thermodynamic properties of isotopic substances. *J. Chem. Soc.*, 12, 562-569, 1947.
- 579 Vergnaud-Grazzini, C.: Non-equilibrium isotopic compositions of shells of planktonic foraminifera in the
580 Mediterranean Sea. *Palaeogeogra., Palaeoclimatol., Palaeoecol.*, 20, 263-276, 1976.
- 581 Vinayachandran, P.N., and Shetye, S.R.: The warm pool in the Indian Ocean. *Proc. Indian Acad. Sci. (Earth Planet
582 Sci.)* 100, 165-175, 1991.
- 583 Wu, G., and Berger, W.H.: Planktonic foraminifera: differential dissolution and the quaternary stable isotope record
584 in the west equatorial Pacific. *Paleoceanography*, 4, 181-198, 1989.
- 585 Wycech, J.B., Kelly, D.C., Kitajima, K., Kozdon, R., Orland, I.J., and Valley, J.W.: Combined effects of gametogenic
586 calcification and dissolution on $\delta^{18}\text{O}$ measurements of the planktic foraminifer *Trilobatus sacculifer*. *Geochem.
587 Geophys. Geosys.*, 19, <https://doi.org/10.1029/2018GC007908>, 2018.